9-1-2009

Activity-Aware Electrocardiogram-based Passive Ongoing Biometric Verification

Janani C. Sriram
Dartmouth College

Activity-Aware Electrocardiogram-based Passive Ongoing Biometric Verification

Dartmouth Computer Science Technical Report TR2009-655

A Thesis

Submitted to the Faculty

in partial fulfillment of the requirements for the

degree of

Master of Science

in

Computer Science

by

Janani Sriram

Dartmouth College

Hanover, New Hampshire

September 2009

Examining Committee:

(chair) Tanzeem Choudhury

David Kotz

Devin Balkcom

Abstract

Identity fraud due to lost, stolen or shared information or tokens that represent an individual's identity is becoming a growing security concern. Biometric recognition - the identification or verification of claimed identity, shows great potential in bridging some of the existing security gaps. It has been shown that the human Electrocardiogram (ECG) exhibits sufficiently unique patterns for use in biometric recognition. But it also exhibits significant variability due to stress or activity, and signal artifacts due to movement. In this thesis, we develop a novel activity-aware ECG-based biometric recognition scheme that can verify/identify under different activity conditions. From a pattern recognition standpoint, we develop algorithms for preprocessing, feature extraction and probabilistic classification. We pay particular attention to the applicability of the proposed scheme in ongoing biometric verification of claimed identity. Finally we propose a wearable prototype architecture of our scheme.

Acknowledgments

This dissertation is the outcome of an enriching and often overwhelming two years. I am glad to take away a diverse set of learning experiences, be it coding with a vengeance, writing a scientific paper, giving coherent talks, team work, or grappling with coursework, insofar as I could achieve across nine eventful school terms and caffeine-fueled all-nighters.

I take immense pride in having the wonderfully unique privilege of being guided by two exceptional computer scientists – Prof. David Kotz who set me on the path that culminated in this dissertation and Prof. Tanzeem Choudhury for shaping my experiments into a structured body of research. They taught me a great deal and I sincerely thank them for their invaluable creative insights. I am also deeply grateful for the stimulating discussions with the other members of the Sensemed group - Minho Shin, Anand Rajan, Manoj Sastry and Mark Yarvis.

The research presented in this dissertation was supported by grants from Intel Corporation, by the U.S. Department of Commerce Award Number 60NANB6D6130, and by the U.S. Department of Homeland Security under Grant Award Number 2006-CS-001-000001. The statements, findings, conclusions, and recommendations do not necessarily reflect the views of the sponsors. I sincerely thank all the sponsors for generously funding our research and particularly Intel Corporation,OR, for their active collaboration.

Dartmouth is a treasure trove of brilliance in computer science and I consider myself fortunate for having the opportunity to be acquainted with some of its brightest minds. Working with Prof. Tom Cormen during my first term was a wonderful experience. I was humbled by the intuitive manner in which he fostered fundamental computer scientific thinking. Admittedly, I learnt more from his course than I ever helped teach. I am proud and grateful for my interactions with Prof. Andrew Campbell, whom I greatly admire, and I sincerely thank him for his warm support and guidance. I must also express my thanks and absolute admiration for Prof. Prasad Jayanthi. Getting to know him was among the most

rewarding experiences at Dartmouth. I also thank all the other faculty members for being incredible influences and fostering a collaborative environment for research and learning.

Being in the CS department at Dartmouth, I had the immense advantage of an outstanding student body and excellent minds to bounce off ideas. I am extremely grateful for the friends I made here at Hanover, who made this a great place to be in, even in the Winter. I also enjoyed my interactions and group meetings with my lab-mates in Lab241 and the Sensor Lab who were an absolute pleasure to be around. I must thank them and all other volunteers for their participation in my research.

Our department definitely has the coolest, most helpful administrative folks a Grad student could ask for. I must thank them for making every tiny little aspect of paperwork, or technical snags so much more easier. I am also very grateful to my International Student Advisor, Mr. Ken Reade, and the International Office at Dartmouth, who were always there to grease the wheels.

I cannot even begin to thank my big bunch of wonderful friends, who absolutely rock, and whose constant presence I sorely miss, Lak and Mad for being splendid big sisters, my brother-in-law whom I could always turn to for help, my extended family who made for such great visits, and Abi, for being a pillar of support through the best and worst of days.

This dissertation is dedicated to my fabulous parents, to whom I am most thankful, for their unswerving love and care.

Contents

List of Figures

List of Tables

Chapter 1

Introduction

The goal of this thesis is the design, development and implementation of algorithms to demonstrate the potential of the human electrocardiogram, combined with the additional modality of accelerometry, to be used in robust, passive, ongoing biometric verification. This is viewed as a pattern recognition problem and the data representation, feature extraction and probabilistic matching are investigated in detail. The novelty of the approach is the use of an additional modality to account for intra-subject variability thereby improving the robustness of the system without loss of detail.

The term *biometrics* is used to refer to measurable physiological or behavioural characteristics of a human subject that can be used to make a probabilistic decision about his/her identity [41, 2]. Biometric recognition operates in one of two modes: the *identification* of a subject as one of those enrolled with the biometric system (a multi-class classification problem) and *verification* of claimed identity (a binary classification problem). *Enrollment* of a subject involves the capture of biometric data, using one or more sensors from that subject, to construct a reliable biometric template of unique descriptors or features, derived from the subject's data, that will serve as the digital representation of

the subject's identity. Any subsequent data from that subject (or any other) presented for verification (or identification) will be matched against the biometric template of the claimed subject (or every subject enrolled with the system).

Biometrics schemes -*what you are/do*, offer several strategic benefits over traditional technologies such as passwords -*what you know* and ID cards - *what you have*. They cannot be misplaced, forgotten or stolen and can be used to ensure physical presence at the point of identification or verification and, thereby, are difficult to repudiate or forge. However, they present some inherent shortcomings. In order to be useful, a biometric characteristic must be sufficiently unique and permanent. How then would a user *cancel* a compromised biometric? For instance, if an attacker obtains a copy of a subject's fingerprint and proceeds to make moulds or even photocopies from these prints, he can potentially use them in a vulnerable system that accepts fingerprints [37]. These concerns lower the general acceptability of biometrics and any biometric system should take adequate measures to protect user privacy. Another cause for concern is that if recognition is performed only once, an imposter can continue undeterred after he manages to circumvent it once. A potential solution is to identify/verify repeatedly over time. But in the case of biometrics that require active participation by the subject, this can be greatly frustrating. In this proposal, we propose a ECG-based biometric scheme that presents many desirable features to address these concerns.

Chapter 2

Motivation

A survey by the United States Federal Trade Commission suggests that approximately 10.1 million U.S. adults discovered that they were victims of some form of ID theft in 2003 and a longitudinal update to the survey revealed that this number had dropped only by a little more than a million in 2006 [21]. With growing concerns about falsification, the collective interest in the use of biometric data as one's digital identity continues to rake up public fancy. Biometric identification/verification offer several benefits over other schemes - most important of which is the convenience of use without having to, say, remember a password or carry an RFID token. Since biometrics are constructed from physical and behavioural traits of a person they preclude the transferability of access. While giving away a password or RFID token seems easy enough, transferring biometric data presents some challenges. This desirable property of biometric data opens up several potential applications, such as remote health monitoring that is considered as a case study for this thesis. Biometric identification/verification is not, however, a panacea for the security risks that plague heavy reliance on 'what one knows' and 'what one has' and each biometric scheme has its potential pitfalls.

The human ECG-based biometric offers several desirable properties. First, the ECG is not strongly permanent nor easily falsifiable. It also inherently provides subject liveness assurance. Being behaviour-based, the ECG biometric is coupled with the different types of algorithms that process it and is not widely interoperable. Thus, there is very little room for abuse of compromised biometric templates beyond the intended application scope. Finally, the ECG, while sufficiently permanent and unique for use in biometric applications, is also not as strongly permanent or unique as some other biometrics such as fingerprints, iris scans and so forth [60, 25, 22]. However, due to the large intra-subject variability we focus our efforts in developing an ECG-based biometric scheme for use in robust, ongoing, passive verification. The fundamental drawback of such an approach is the intricate and intrusive setup required to collect the ECG using the standard 12-lead procedure [58, 20]. Hence we demonstrate our approach using a single lead ECG collected from a wearable sensing system (see Section 5.1).

Ongoing verification is very useful in several applications that could benefit from subsequent checks after the point of verification to ensure that the claimed identity is still the one under consideration. This problem has been recently explored using different types of biometrics such as face, speech and gait [31, 32, 54, 15]. We describe in our next section, one such application - remote health monitoring, where such a scheme would be easily implemented and desirable using the modalities under consideration.

Health Monitoring - A Case Study: Remote health monitoring systems that gather health data using wearable sensors have immense potential to improve the quality of life of different kinds of people such as those suffering from chronic illnesses, those seeking to change behavior such as smoking, those seeking diagnosis for specific medical conditions etc. [33, 30, 40, 48, 34, 10]. A fundamental problem with remote health monitoring is the

issue of *patient identification* - do sensor data belong to the desired patient? We require that the proof for user authentication is non transferable since the authentication mechanism will not be reliable enough if based on something that the user knows or possesses since a cheating user can potentially pass on both to someone else. Hence a reliable authentication mechanism should be coupled with something the user is/does i.e., biometrics.

A one-time identification/verification step presents the risk of unauthorized use by an authorized user, such as, a patient giving the sensor to someone else to wear. Another potential risk involved is that an attacker can continue undisturbed if he manages to bypass the initial identification/verification step. These risks may lead to incorrect medical or financial decisions using the subsequent data. Ongoing biometric recognition is desirable for all available samples of sensor data to ensure that subsequent data belongs to the desired patient.

For usability we require that the biometric recognition process is unobtrusive or passive and does not require active participation by the individual to be identified (such as speech recognition), since it has to be performed often.

Unique, permanent and extensible biometric data such as that used to strongly identify individuals (e.g., fingerprints) give rise to privacy concerns. User anxiety about privacy can be mitigated if biometric data that is sufficiently unique for use in permanent identification is not collected.

From the above design guidelines we have the problem of patient authentication using ongoing biometric verification with passive, poor biometrics in order to make a narrow probabilistic judgement about the claimed identity of the participant. Our approach is to investigate the potential of using multiple modalities of health data (ECG and accelerometry) collected in the context of remote health monitoring for verifying the identity of the sensor wearer. This follows from our hypothesis that a physiological signature can

be constructed from the patient's sensor data to probabilistically verify whether subsequent sensor data is representative of that physiological signature.

A *physiological signature* using these modalities can potentially pave the way for an ongoing, passive biometric verification scheme that is not expected to be permanently distinctive, but is sufficiently discriminatory over a short term. Such a *physiological signature* provides an assurance of vitality of the subject. Biometric systems that do not address this are at risk of falsification by an intruder presenting biometric data of another subject as if it were his own.

We summarize our goals for patient authentication as follows.

- (Non-transferable) the patient should be authenticated based on physiological or behavioural characteristics.
- (Ongoing) the patient should be authenticated throughout the duration of monitoring.
- (Passive) the patient should not be interrupted for repetitive authentications.
- (Privacy-aware) the authentication data should not be sufficiently unique to irrevocably identify the patient.

Chapter 3

Background

The human electrocardiogram reflects the specific pattern of electrical activity of the heart throughout the cardiac cycle, and can be seen as changes in potential difference. The ECG is affected by a number of physiological factors including age, body weight, and cardiac abnormalities. A typical beat in an electrocardiogram (see Figure 3.1) consists of

1. A low amplitude P-wave, representing atrial depolarization,
2. The QRS complex of much higher amplitude than the P-wave, representing ventricular depolarization
3. A T-wave of smaller amplitude and larger duration than the QRS complex, representing ventricular repolarization.

3.1 Acquisition

The non-invasive procedure to obtain the electrocardiogram is to record the body surface potential using skin electrodes. Electrode-skin impedance is reduced using an electrically conductive fluid, typically electrode gel and in some cases even water, for e.g., Polar

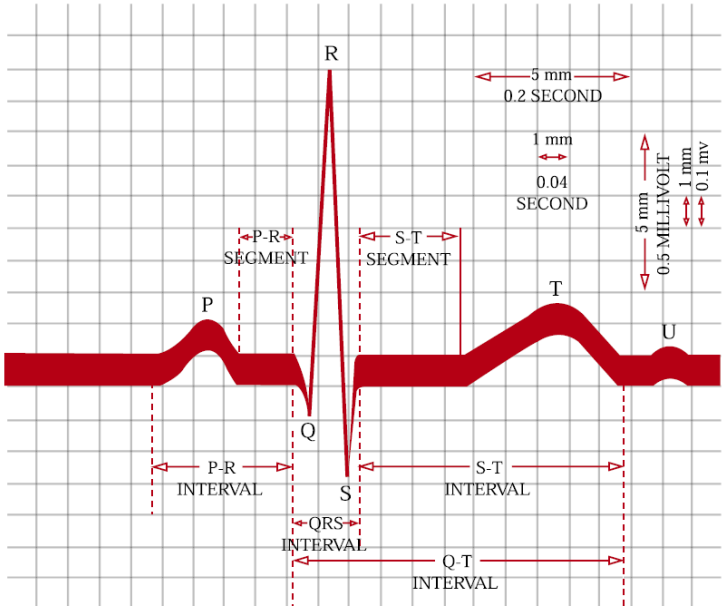

Figure 3.1: The normal clinical features of the electrocardiogram in terms of wave timings and amplitudes. Each square on the grid represents a resolution of 0.04s×0.1mV. Adapted from MIT Open Course Ware material ©2004 MIT-OCW.

Wearlink chest strap. The potential difference seen between a pair of electrodes constitute a single lead of ECG. Different lead configurations are possible depending on the placement of the electrodes leading to different correlated views of the electrical activity of the heart. The choice of leads is based on different diagnostic needs. We refer the reader to Frank et al. [20] and Welinder et al. [58] as a starting point for further consideration. For the purposes of this thesis we assume a single chest lead in Lead I configuration (electrodes placed on left and right arms).

3.2 Analysis

The human ECG exhibits different types of quasi-periodic trends as well as beat-to-beat and interbeat abnormalities that may be responses to physiological stimuli, such as, physical or mental stress or signal artifacts. A general methodology for ECG analysis

from a pattern recognition perspective consists of preprocessing, feature extraction and classification. The ECG trace is, first, filtered to remove noise sources, then segmented into heartbeats (a sequence of P-QRS-T waves) or conveniently sized windows. In the former case morphology based timing and amplitude features can be extracted from the sequence of beats and in the latter case spectral analysis reveals the significant trends in the ECG trace. The extracted features are then used as inputs to different types of diagnostic classifiers [28, 43, 46, 14]. For biometric identification/verification we need to extract a set of features that describe the unique patterns found in the ECG of different individuals.

3.3 Sources of Variability

We can view the intra-individual variability in two broad categories - acquisition artifacts and arrhythmias. In comparison to different forms of invasive electrocardiography, the surface ECG serves as a convenient and immensely useful diagnostic tool. But it also has higher susceptibility to noise, particularly electrode contact noise and motion artifact in the face of activity. Overlooking the possible biases and artifacts due to the signal acquisition methods such as lead configuration, patient activity without activity annotations etc. leads to erroneous analysis. The second category of variability is due to transient changes in the underlying physiology such as activity induced heart rate increase, respiration induced arrhythmia etc. It has been reported that several morphological characteristics vary with increasing heart rate such as the QT interval, ST level, QRS width, P ,Q, and T - wave heights etc [18, 36].

3.4 Potential as Biometric

The ECG signal from different individuals conforms to a fundamental morphology and is also known to exhibit several personalized traits, such as relative onsets of the various peaks, beat geometry, and responses to stress and activity. The persistent inter-individual variability in the ECG is reported to be due to a variety of factors such as age, gender and lifestyle choices (caffeine intake, BMI, physical exercise etc.) [25, 22, 24]. This inter-individual variability frustrates clinical diagnostic algorithms but is manifested as unique patterns that can be leveraged to discriminate individuals. However, changes in factors causing long term variability in the ECG (for e.g., ageing, increased physical exercise), prevents permanent and unique identification of a person. This is easily dealt with by periodic update of biometric profiles and actually serves as an added benefit in mitigating concerns about privacy and revocability of biometrics [45, 3].

The ECG, as a biometric, thus offers several clear benefits, such as universality, difficulty of falsification, inherent liveness assurance, and robustness to environmental factors since the heart is well protected in the thoracic cavity. The short-term stability of the ECG signal was reported by Wuebbeler et al., by collecting data from healthy subjects over 1 to 118 days [60]. An ECG-based biometric system offers significant promise, therefore, but we need to understand and account for the sources of significant intra-individual variability. These variations include physiological responses to stimuli such as stress and activity, and signal artifacts due to movement. In this thesis, we introduce an additional sensor – an accelerometer – to further investigate the effect of measurable body acceleration on the ECG-based authentication of an individual. We construct a biometric profile that contains more information than ECG-only approaches, build classifiers for identification or verification of claimed identity, and finally evaluate the improvement in performance during

various conditions and activities.

Chapter 4

Related Work

Several recent studies have investigated the potential of using physiological signals such as the Electrocardiogram (ECG), Photoplethysmograph (PPG), Electroencephalogram (EEG) etc. for biometric identification and verification [15, 17, 9, 1, 23, 26, 44, 52, 57, 59, 11, 53, 44, 27]. The benefit of using such physiological biometrics is the difficulty of falsification and assurance of liveness of the subject. Such systems, however, present significant intrasubject variability and hold no promise of a reliable identification/verification scheme in uncontrolled conditions unless provided with a means of accounting for the variability. This section will introduce some of the significant papers in the realm of ECG based biometric identification/verification, thus establishing a context for the approach proposed in this thesis. We highlight the following points in each approach - features extracted, experimental setup, robustness to variability and reported results.

An initial review of related work reveals two broad categories of feature extraction techniques for the ECG data depending on whether segmentation of the ECG trace into heartbeats is required. In *fiducial* feature extraction, points of reference called *fiducial-points* are marked along the time series. The fiducial points are derived from known mor-

phological characteristics of the human ECG and the extracted features are typically some combination of time and amplitude differences between these fiducial points. The problem with the fiducial analysis is that errors in localization of wave boundaries lead to incorrect identification of fiducial points. Other *non-fiducial* approaches have been proposed to mitigate this issue by using some form of spectral analysis.

Biel et al.'s work in automatic human identification was one of the earliest to introduce an approach for using the human ECG as biometric [4]. A 12-lead ECG system, the Siemens ECG Megacart was used to obtain the data from 20 subjects at rest over a period of six weeks. The features extracted were a set of 30 standard clinical diagnostic characteristics for each lead. The authors use correlation analysis to reduce the dimensionality of the feature vector and finally classification of subjects was performed by a Soft Independent Modeling of Class Analogy (SIMCA) classifier. Different combinations of features and leads were studied with a best reported accuracy of 100% for 50 test samples. The approach, however, relies on the availability of standard diagnostic data from the ECG equipment rather than a general feature-extraction procedure. This is a major drawback of the approach since such computation is expensive for sensors that report only the ECG measurements and is also superfluous since many diagnostic features are not useful as biometric features.

Israel et al. then proposed an approach for pre-processing, feature extraction and classification of individuals based on their ECG traces[26]. The authors collected data from 29 individuals while performing seven tasks causing varying levels of mental stress. They detect fiducial points and use normalized temporal distances between the fiducial points as features. They then perform feature reduction by Wilk's lambda and classify using discriminant analysis. The authors set out to establish that the proposed ECG features are invariant to state of anxiety with a 98% classification performance, and hence, constitute a valid biometric. But the tasks involve 2 minutes of stressful activity with minimal physical

movements and cannot be used in a scenario where other physical activities would introduce further variability. The paper also does not address the issue of reliable fiducial point detection and potential degradation of classification performance due to errors in localization of heart beat boundaries. The authors also include an analysis of the effect of sensor placement. In a subsequent paper by one of the authors, the proposed ECG features were used together with face recognition in a multimodal biometric identification system [27]. For 35 individuals, voting fusion between face and ECG performed the worst with 60% accuracy. The best performance was achieved using attribute level fusion and feature vector concatenation with 99% accuracy. For decision level fusion only a marginal improvement in accuracy was achieved over face recognition alone (94%).

Shen et al. proposed a biometric identification scheme using 7 features from the most invariant part of the heartbeat, the QRS complex together with the T-wave [52]. The scheme performed with an accuracy of 95% for a template matching classifier and 80% for a DBNN over a group of 20 individuals from the MIT-BIH database [39]. By combining the outputs of the two classifiers, the authors achieve an accuracy of 100%. The authors select a set of representative heartbeats for each subject and test against a subset of remaining heartbeats. The automatic segmentation of an ECG trace into heartbeats is, however, one of the significant sources or error.

Wang et al. were the first to propose an approach that did not entirely rely on fiducial based features by combining a set of analytic features' derived from fiducial points with 'appearance features' obtained using PCA and LDA for feature extraction and data reduction [57]. The accuracy for 13 subjects was 84% using analytic features alone and 96% using LDA with K-NN. The combination of the types of features was used to achieve 100% accuracy.

Several non-fiducial approaches have been proposed that use some form of frequency-

level analysis. Plataniotis et al. have proposed an approach that uses Autocorrelation analysis coupled with Discrete Cosine Transform of the autocorrelated signal and does not require segmentation of the ECG trace into heart beats [44]. The approach achieves close to a 100% accuracy for a database of 14 subjects.

Chan et al. proposed another non-fiducial feature extraction framework using a set of distance measures including a novel wavelet transform distance [9]. Data was collected from 50 subjects using button electrodes held between the thumb and finger. The wavelet transform distance outperforms other measures with an accuracy of 89%.

Studies investigating the variability of ECG traces due to activity indicate that the reliability of the ECG based biometric scheme would degrade with varied conditions such as activity or stress that causes intra-subject variance (physiological or artifact) [56, 47, 55, 19] . Hence these approaches are unsuitable for the desired ongoing verification of identity when the human subject is not at rest throughout the duration of monitoring. The goal of this thesis is to address this gap by introducing the additional modality of accelerometry to account for such variability and investigate the performance of ECG as biometric aided by accelerometry.

Table 4.1 highlights the significant features of some of the related approaches with our scheme. It should be noted that we cannot realistically compare the accuracy of different schemes due to several interpretation issues such the number of test samples required to identify a subject, experimental setup and data collection methodology.

Reference	Feature	Method	Subjects	Activity	Acc
Biel [4]	Fiducial	PCA	20	No	100%
Shen [52]	Fiducial	Template Matching+DBNN	20	No	100%
Israel [26]	Fiducial	LDA	29	No	98%
Wang [57]	Both	KNN+LDA	13	No	96%
Chiu [11]	Non-Fiducial	Wavelet Distance+LDA	35	No	100%
Chan [9]	Non-Fiducial	wavelet DM	50	No	89%
Ours	Both	KNN+Bayesian	17	Yes	88%

Table 4.1: Comparison of related work with our scheme. The accuracy values represent the percentage of subjects who are correctly identified for a majority of their test samples.

Chapter 5

Methodology

Biometric recognition (identification or verification) is viewed essentially as a pattern-recognition problem; in this section we outline the preprocessing, feature extraction, and classification steps. We seek to investigate the performance for two different kinds of classifiers: the K-Nearest Neighbor (which classifies using a multimodal feature vector) and the Bayesian network classifier (which separates the activity features from that of the ECG features into 2 nodes).

Our approach is aimed at tackling intra-subject variability robustly for verification. We begin our investigation by evaluating the *identification* performance to demonstrate the potential of the proposed scheme and to establish a baseline for comparison with existing approaches. We evaluate our method's performance using data collected using wearable sensors from 17 volunteers during varied activity sessions over different days as described in Section 6.1.

5.1 Sensors

We use the SHIMMER platform developed by Intel Digital Health Advanced Technology Group. The SHIMMER[1] is a compact sensing platform with an integrated 3-axis accelerometer. SHIMMER runs the TinyOS operating system and integrates (via custom cabling) to a commercially available Polar WearLink Plus ECG chest strap[2] . A 3-Axis accelerometer is mounted on the SHIMMER's base sensor board, and ECG sensing is available by means of a 20-pin internal expansion connector on the baseboard. The ECG add-on board provides connectors for 4 standard leads and estimates the corresponding 2-channel ECG vectors from which other vectors can be computed. We used the Polar Wearlink chest strap and two compatible connectors to obtain a single lead of ECG (Lead I configuration). The Polar Wearlink chest strap has electrode patches embedded into the fabric, which transmit the differential voltage signal to the connectors plugged into the strap. The strap is wet before wearing, with cold, running water, to reduce skin-electrode friction.

SHIMMER runs the TinyOS operating system. We developed a NesC application to periodically read the available samples, prepare the packet as a delimited ASCII string and forward it over a serial Bluetooth link. For our initial data collection we used the BioMOBIUS software to send commands to and stream data from the SHIMMER [6].

5.2 Preprocessing and Feature Extraction

We segment the ECG and accelerometer traces into 400-sample windows (approximately 4 seconds of data) to obtain the feature windows $w_1, w_2, \ldots, w_n$. We use $w_i(j)$ to denote the j^{th} sample of feature window w_i.

[1] `http://shimmer-research.com/`

[2] `http://polarusa.com/`

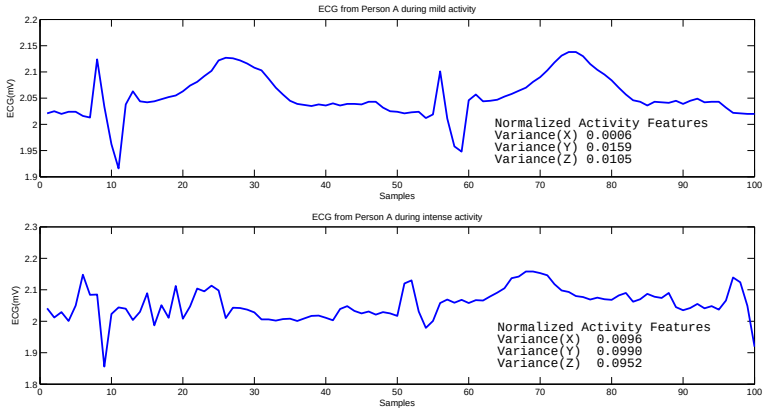

Figure 5.1: The ECG of a healthy subject at the beginning of exercise activity (above) and signal distortions due to motion artifact introduced as the subject proceeds to perform intense exercise activity (below).

We chose the size of the feature window so that multiple heart beats are present within a given window (at least 4 in our case). We attempt to reduce the impact of misclassified R-peaks by averaging beat features within the window rather than relying on features extracted from a single beat. Although, this method introduces a time lag of 4s, we can reasonably assume that change of activity or person takes longer than 4s. We use the notation w_i^a and w_i^e to denote the accelerometer data and ECG data respectively within the i^{th} feature window.

Any raw ECG trace collected using non-invasive surface electrodes usually has several artifacts, notably a low frequency baseline drift due to respiratory effects, electrode contact noise, and motion artifacts. Typically this noise is removed by high-pass or moving-average filtering techniques [47, 38, 12]. Since we collect our datasets during exercise, including durations of high-intensity activity, the ECG trace was also corrupted with the more troublesome motion artifact noise whose spectrum overlaps the ECG band (see Figure 5.1). The corresponding signal distortions cannot be easily eliminated by filtering.

We perform baseline correction before non-fiducial feature extraction. We employ

an adaptive, beat-based linear interpolation approach to estimate the baseline from the line joining the Q-minima. The estimated baseline is then subtracted to align all beats within a window. Baseline correction introduces some sharp discontinuities within the window, so before non-fiducial feature extraction we employ a high pass filter with coefficients adapted from [42].

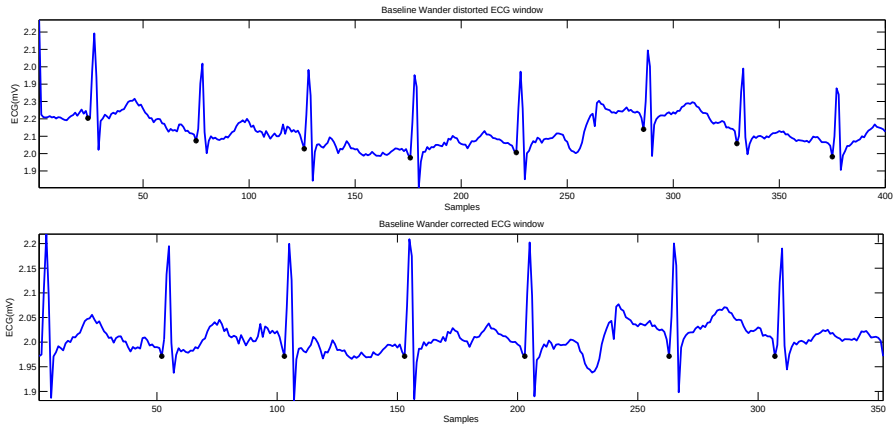

Figure 5.2: Baseline wander in the ECG window (above) introduced due to respiration is corrected adaptively by removing the estimated baseline formed by linear interpolation of the Q-minima (below).

We adopt a combination of two commonly used analyses of the pre-processed ECG trace to obtain a feature vector as shown in Table 5.1. We select the dimensions of different features empirically. We extract a combination of the two types of ECG features, fiducial and non-fiducial, from windows of the pre-processed signal. The final feature vector is shown in Table 5.1.

5.2.1 Fiducial Analysis

Our procedure for beat segmentation and fiducial feature extraction is described in Algorithm 1.

Spline Interpolation: The general morphology of the segmented beats can be rep-

Algorithm 1 Detects the set of beats $\mathcal{B}$ and the sets of QRS markers, q,r,s, using an existing QRS detector [12]

1: The detected R-peaks are denoted by a set r of sample index-amplitude pairs as $(r_j, w_i^e(r_j))$, for the j^{th} beat of the i^{th} window of the ECG trace.

2: **for all** r_j in r **do**

3: Search downhill from each R-peak to locate the Q and S minima as $(q_j, w_i^e(q_j))$ and $(s_j, w_i^e(s_j))$. (The normal width of the QRS peak is known to be 100 ± 20ms [12]. We incorporate this fact by searching between ± 6 samples of the detected R-peaks.)

4: Align beat along the detected R-peaks by extracting a sequence of samples of size $\min((r_{j+1} - r_j), (r_j - r_{j-1}))$ so that the R-peaks are centered within the extracted beat segments. Discard if current beat $\mathcal{B}_j$ is incomplete and cannot be centered.

5: Normalize the beat by clamping the R-peaks to 1 and the Q-minima to 0.

6: **end for**

7: Discard beats corresponding to poorly detected fiducials that do not contain Q and S minima within the assumed search interval.

8: **return** $\{\forall j\ \mathcal{B}_j, (q_j, w_i^e(q_j)), (r_j, w_i^e(r_j)), (s_j, w_i^e(s_j))\}$

	Feature
F1-F20	First 20 normalized AC co-efficients
F21-F41	Spline interpolant
F42	Normalized slope $\frac{QR}{QR+RS}$
F43	Normalized slope $\frac{RS}{QR+RS}$
F44	R-R interval
F45-F50	Accelerometer X,Y,Z means and variances

Table 5.1: Feature vector representing the biometric profile of an individual

resented by a set of features derived from the relative positions and heights of different fiducial points. However, due to the presence of beats exhibiting subtle morphological variabilities as well as erroneous waveforms showing marked deviation from normal waveform (for e.g., physiological artifacts such as ectopic beats, signal artifacts such as noisy in-band signals etc.) we employ piecewise polynomial approximation to represent the underlying morphology. Thus, we seek to minimize our dependence on the localization of other fiducial points which are more susceptible to noise as compared to the R-peaks. Our choice of interpolant is the natural cubic spline, described below in further detail. The cubic spline is commonly used in ECG morphological analysis for upsampling and smoothing of beats [35, 16, 51, 29, 13]. For a given set of $(n+1)$ points $(x_0, x_1 \ldots x_n)$, the i^{th} 'piece' of the cubic spline is defined by the polynomial function [49],

$$y_i(t) = a_i + b_i t + c_i t^2 + d_i \tag{5.1}$$

Where $t\epsilon\,[0,1]$ and $i = 0, 1, \ldots (n-1)$.

$$y_i(0) = x_i = a_i \tag{5.2}$$

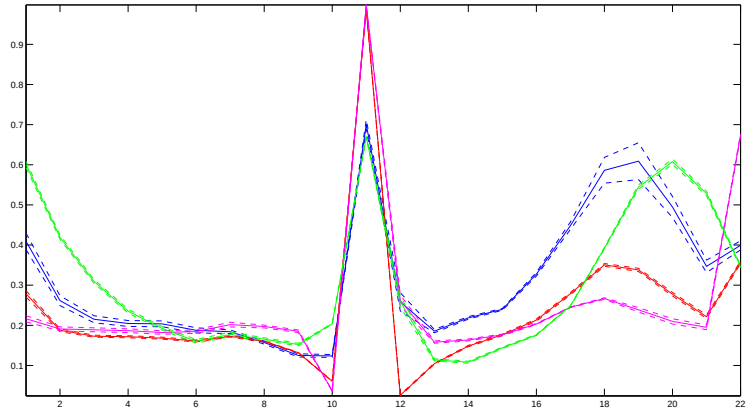

(a) Normalized Spline interpolant for 4 different subjects over select samples (means and variances)

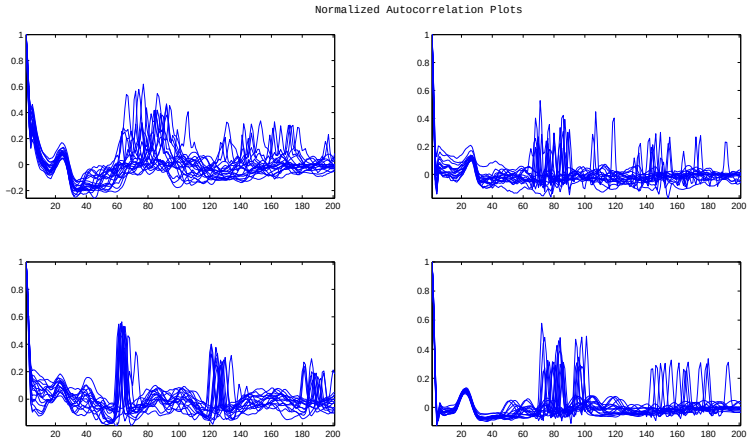

(b) Normalized Autocorrelation for 4 different subjects over select samples (only the tail portion shown)

$$y_i(1) = x_{i+1} = a_i + b_i + c_i + d_i \tag{5.3}$$

By imposing the additional constraints that the second derivative at the endpoints are zero, we obtain the y, the C_2 continuous (continuous up to second derivative) natural cubic spline.

Note that the normalized beats within a window have different periods since the adaptive segmentation in step 4 of Algorithm 1 is based on the distance between the R-peaks of the beats on either side of the current one. The underlying beat morphology is obtained from the mean spline (cubic) interpolant (F21–F41) of the beats within the feature window.

In addition, we extract the mean R-R peak distances (F44) and the slopes QR (F42) and RS (F43). The RR-interval is normalized using the equation $\frac{x-l}{u-l}$ where x represents the current value and u and l represent bounds on the RR-interval (25 to 300 samples representing a heart rate range of 20 to 240 beats per minute). The slope features are normalized using the sum of the two slopes.

At the end of this stage we have a set of features that capture the underlying beat geometry and the activity induced variations. In particular, feature F44 models the intra-individual variations caused by physiological response to activity in the form of increased heart rate. Our set of fiducial features is a subset of those found in literature [4, 26, 52] with improved normalization and a novel adaptive beat-segmentation approach based on activity induced heart-rate changes.

5.2.2 Non-fiducial Analysis

The presence of noise in the signal often leads to errors in beat segmentation of the ECG trace. So we complement the feature vector with a set of *non-fiducial* features that are less sensitive to the inaccuracies in beat segmentation [44, 9, 11].

Autocorrelation features have been used for their ability to extract redundancy in the ECG signal without requiring preprocessing of the electrocardiogram to obtain the significant points and segments. The Autocorrelation function of a signal represents how well the waveform correlates with a time shifted version of itself i.e., its periodicity. The maximum time-shift that is considered is denoted by MAXLEAD. For a sequence, x, of n

samples representing the i^{th} ECG window $x = w_i^e$, the autocorrelation function is defined as

$$R_{xx}(m) = \sum_{i=0}^{n-|m|-1} x(i)x(i+m) \tag{5.4}$$

where lags $m = 0, 1 \ldots MAXLEAD$ where $MAXLEAD \ll n$

For different types of time-series models, the maximum number of lags (or leads, interchangeably) that are statistically relevant vary. Plataniotis et al. found that lags over 200ms (20 samples) give poor performances [44]. We further verified this using MAXLEADS of 2s (200 samples) and observed that coefficients beyond, approximately, the first 20 samples, are not useful (See Fig. 5.2).

We use the normalized autocorrelation coefficients of each w_i^e as described by Plataniotis et al. [44]:

$$\tilde{R}_{xx} = \frac{R_{xx}(i)}{R_{xx}(0)}, \text{where } i = 1, 2 \ldots MAXLEAD. \tag{5.5}$$

We use the first 20 normalized coefficients ($MAXLEAD$=20) for each ECG window (n=400) as our non-fiducial features (F1–F20).

$$\tilde{R}_{xx} = \frac{R_{xx}(i)}{R_{xx}(0)} \tag{5.6}$$

where $i = 2, 3 \ldots MAXLAGS$.

5.2.3 Accelerometer

The triaxial accelerometer is a device that measures the acceleration along the x, y, and z-axes (see Figure5.3). By measuring the dynamic acceleration of the device we can make inferences about the activity of the person wearing the sensing device. We first zero-mean the signal by subtracting the mean of the entire trace. Then for each axis, we

compute the mean and variance of the window w_i^a. The classifiers use these features to discriminate between different activities.

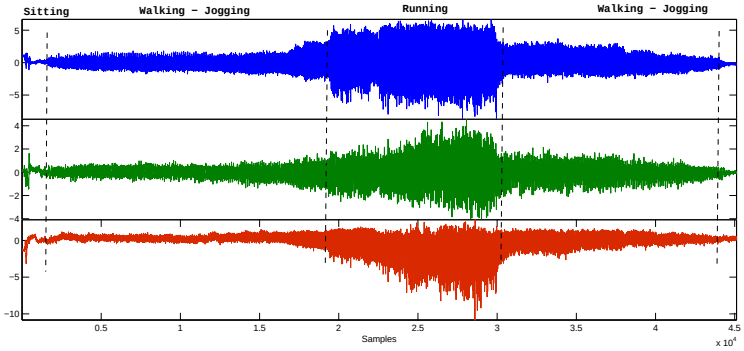

Figure 5.3: The x,y and z-axes acceleration for the various activities performed by subjects.

5.3 Classification

The goal of classification is to identify a subject or to verify an identity claim from the sensor observations. We investigate the performance of two types of classifiers: K-Nearest Neighbor (KNN) and Bayesian network (BN).

5.3.1 K-Nearest Neighbour

We first measure the benefit of incorporating activity information for identification using simple KNN classifiers. We trained two KNN classifiers: an activity-aware classifier, which uses the multimodal feature vector (F1–F50), and an activity-unaware classifier which uses the unimodal feature vector (F1–F44). KNN typically uses Euclidean distance as its distance metric. We combine estimated pairwise correlation distances for features F1–F20 and F21–F42 and Euclidean distances for all other features to obtain a modified KNN

classifier.

Suppose we have n samples such that the i^{th} sample is represented as $f_i = (f_{i1}, f_{i2}, \ldots, f_{im})$, $i = 1, 2, \ldots n$ and m be the number of features, i.e., 50. The distance, d, between samples f_i and f_j is calculated as follows,

$$f_{ia} = (f_{i1}, f_{i2}, \ldots f_{i20})$$

$$f_{ib} = (f_{i21}, f_{i22}, \ldots f_{i42})$$

$$f_{ic} = (f_{i43}, f_{i44}, \ldots f_{i50})$$

$$d_1(f_{ia}, f_{ja}) = 1 - \frac{(f_{ia} - \bar{f_{ia}})(f_{ja} - \bar{f_{ja}})'}{\sqrt{(f_{ia} - \bar{f_{ia}})(f_{ia} - \bar{f_{ia}})'}\sqrt{(f_{ja} - \bar{f_{ja}})(f_{ja} - \bar{f_{ja}})'}}$$

$$d_2(f_{ib}, f_{jb}) = 1 - \frac{(f_{ib} - \bar{f_{ib}})(f_{jb} - \bar{f_{jb}})'}{\sqrt{(f_{ib} - \bar{f_{ib}})(f_{ib} - \bar{f_{ib}})'}\sqrt{(f_{jb} - \bar{f_{jb}})(f_{jb} - \bar{f_{jb}})'}}$$

where $\bar{f_i}$ denotes the sample mean.

$$d_3(f_{ic}, f_{jc}) = (f_{ic} - f_{jc})(f_{ic} - f_{jc})'$$

$$d(f_i, f_j) = d_1(f_{ia}, f_{ja}) + d_2(f_{ib}, f_{jb}) + d_3(f_{ic}, f_{jc})$$

The additional correlation distance metric represents the similarity in the shapes of two curves. We evaluated the performance of both the Euclidean-distance based KNN and the modified-KNN (xKNN) classifiers.

5.3.2 Bayesian Framework

Our hypothesis is that explicit modeling of activity states will lead to better recognition performance. We developed two Bayesian network classifiers to allow us to evaluate that hypothesis (shown in Figure 5.6).

Suppose we have N persons whose identity P is given by the labels $p = p_1, p_2, \ldots, p_N$. The biometric profile for a person p_i is a set of m ECG feature vectors $e = \langle e_1, e_2, \ldots e_m \rangle$ and the corresponding activity feature vectors $a = \langle a_1, a_2, \ldots a_m \rangle$. We assume that the ECG features are normally distributed, i.e., $P(E \mid P, A) \sim N(\mu, \Sigma)$, and depends on the person and the activity being performed. The problem of classification is now reduced to that of estimating the parameters of the conditional distributions of Equation (5.7). We discretize the accelerometer features, A, into distinct activity levels H and obtain the Bayesian network (BN) shown in Figure 5.6(a). The joint distribution of the BN is defined as

$$P(P, H, A, E) = P(E \mid P, H)P(A \mid H)P(H)P(P) \tag{5.7}$$

Activity Discretization

The activity levels that are of interest are those of different activity intensities introducing corresponding variations in the ECG signal (see Fig. 5.4). These variations may be due to physiological response to activity such as decrease in RR-interval (increase in heart rate) as well as signal artifacts. The activity levels H were obtained in two ways: from manual annotations and via unsupervised clustering. Manual annotations include three activity levels: still, low-intensity, and high-intensity. We also tested three types of unsupervised clustering techniques: K-means clustering with the Euclidean distance metric, K-means using city block distance and Gaussian Mixture Model (GMM) with diagonal covariance matrices. Ultimately, we chose the GMM which allows soft cluster boundaries and resulted in better performance. Since the manual annotations contained significant human error, there was no reliable ground truth for comparing the activity clustering. So we visually compared the inferred cluster IDs with our manual annotations and found that the inferences were close except for occasional discontinuities (see Figure 5.5).

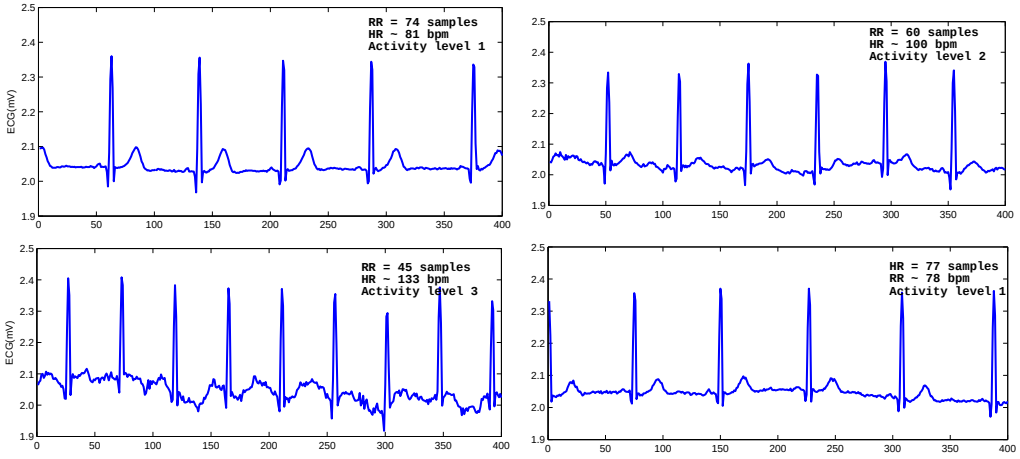

Figure 5.4: Unsupervised activity clustering.

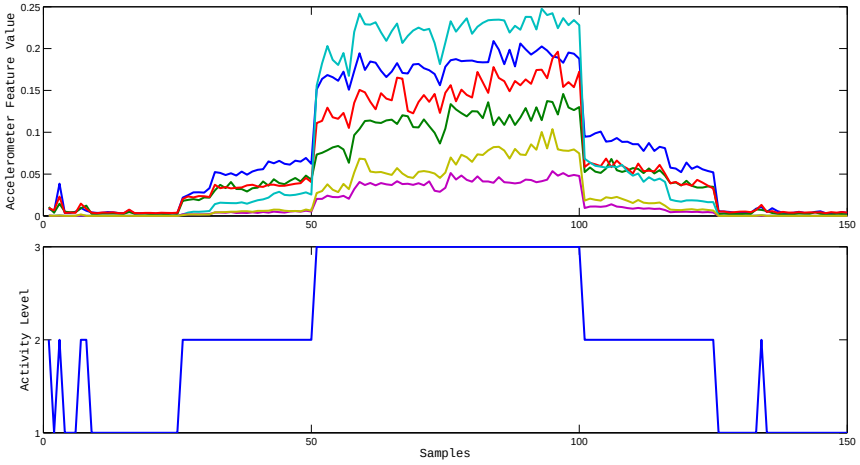

Figure 5.5: Example of unsupervised activity clustering using GMM clustering with 3 activity levels.

Activity-Aware Classification:

During training, we assume that the BN is fully observed. In identification mode the class labels are $p = p_1, p_2, \ldots, p_N$ for N subjects and in verification mode, $p = \{\text{legitimate,imposter}\}$. The hidden node H models the discrete activity labels from clustering (see Figure 5.6). We

perform clustering independently for each subject during training. During testing both nodes H and P were hidden. We used the Bayes Net Toolbox [8] for training and inference. Inference is by a a junction-tree inference engine (exact inference).

During testing, we are interested in estimating the probability distribution of the hidden variable P, conditioned on the accelerometer and ECG features $A = a$ and $E = e$ respectively, i.e.,

$$P(P \mid A = a, E = e) = \sum_{j=1}^{|h|} P(P, H = h_j \mid A = a, E = e) \tag{5.8}$$

The predicted person label p_{pred} is the one that maximizes the posterior probability.

$$p_{pred} = \underset{P}{\operatorname{argmax}} \sum_{j=1}^{|h|} P(P, H = h_j \mid A = a, E = e) \tag{5.9}$$

To evaluate the usefulness of the activity features, we also test an activity-unaware the Bayesian classifier shown in Figure 5.6(b), which uses only the set of ECG features.

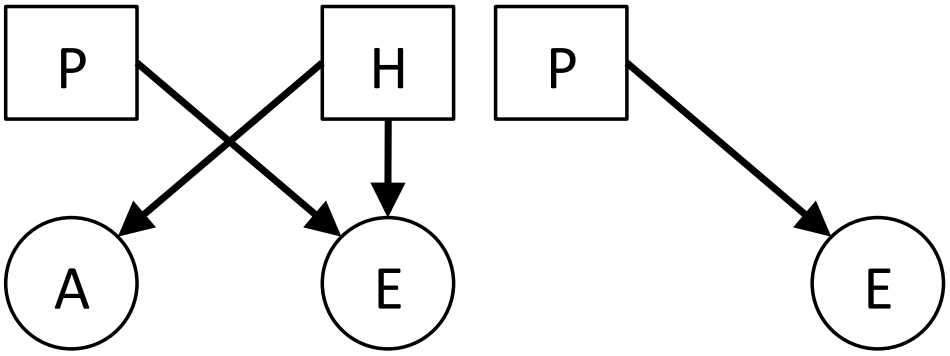

(a) The Activity-Aware Bayesian network - BN and BN.

(b) The Activity-Unaware Bayesian network BN(NA).

Figure 5.6: Nodes: Person ID $p = 1, \ldots, N$ for N subjects. The feature nodes A and E are 6 and 44-dimensional Gaussians respectively. Node H represents the discrete activity labels.

Identification: During identification, the system selects the person with highest marginal probability. The goal of the identification phase is to evaluate the biometric potential of our dataset and processing algorithms.

Verification: During verification we are only interested in accepting or rejecting a claimed identity. One possible approach is to compare the probabilities estimated during identification against a threshold to obtain verification decisions.

Another approach is to perform binary classification using two class labels, $p = \{\text{legitimate,imposter}\}$ – which leads to a more compact probabilistic model and maybe preferable when there are a large number individuals, especially by mobile inference systems.

To build a binary verification model, we need a representative set of imposters for each individual. Selection of imposters has been the subject of much research in related studies of person verification using speech, signatures and other modalities that exhibit significant intra-subject variability [5, 50, 54]. Similarly, such work has also noted variability caused by uncontrollable factors such as emotional state, health or recording conditions. Hence there is a degree of mismatch between test and training data for an individual. We adopt two principles from this body of work: the selection of subject-specific imposters and the pooling of samples from multiple imposters. We describe our verification algorithm in Algorithm 2, in which we denote the training data for persons $p = \{p_1, p_2 \dots p_N\}$ to be $\mathcal{D}(p_1), \mathcal{D}(p_2) \dots \mathcal{D}(p_N)$.

Finally, the system uses the verification score, given as the ratio of true and imposter model likelihoods, to make a decision about a claimed identity p_i:

$$\frac{P(p_i \text{ is a legitimate claimant})}{P(p_i \text{ is an imposter})} \tag{5.10}$$

Since both probabilities are obtained from the claimant's model the proportional score simply serves to exaggerate differences in their probabilities for comparison against a threshold.

Algorithm 2 Training the pooled imposter model for Verification

1: **for all** claimants $p_i \epsilon\ p = \{p_1, p_2 \ldots p_N\}$ **do**
2: select a set of k most confused subjects as imposters $\hat{p} = \{\hat{p_1}, \hat{p_2}, \ldots \hat{p_k}\}$ such that $\hat{p_j} \epsilon\ p$ and $\hat{p_j} \neq p_i$ for any j
3: obtain the legitimate claimant dataset $\mathcal{T}$ as $\mathcal{D}(p_i)$
4: **for** $j = 1$ to k **do**
5: add $\mathcal{D}(\hat{p_j})$ the pooled imposter dataset $\mathcal{F}$
6: **end for**
7: Randomly sample from the pooled imposter dataset such that $\mathcal{T}$ and $\mathcal{F}$ are of equal sizes.
8: Estimate model parameters for p_i, training data $\bar{\mathcal{D}} = [\mathcal{T}, \mathcal{F}]$
9: **end for**

The potential to misclassify subjects who are not represented in the imposter pool is one of the drawbacks of the proposed verification model. But the compact representation and lower computational cost makes it a potentially appealing option. When we tested a dataset of 20 samples on the identification model running on an Intel Core2 Duo machine, it took approximately 0.6 seconds to predict all class labels. A verification decision on the same dataset took around 0.2s.

Combining Multiple Predictions: We refer to the individual prediction for each feature window as window identification/verification. A sequence of window identification/verification decisions are used to make person identification/verification decisions by majority voting. During identification, an entire test sequence is classified as belonging to person p_i if the majority of the predictions are for p_i. During verification, an entire test sequence is verified for a certain claim p_i if the majority of the predictions are verified as

legitimate. For ongoing verification, instead of majority voting over the entire dataset, we evaluate the performance of the classifier as follows,

1. Divide test dataset in chunks of 10 feature windows each.
2. For each chunk if the majority of windows is classified as legitimate, the claimant is considered legitimate. If not the claimant is an imposter.

Chapter 6

Experiments and Results

To test the feasibility of our approach, we collected data from 17 volunteers under different activity conditions and across different days. To make it easier to compare with related approaches, we present the *identification* performance of the classifiers in addition to the verification results.

The goal of this thesis is to develop a robust ECG-based biometric scheme for use in ongoing verification of claimed identity. We, therefore, cannot expect users to remain at rest throughout the duration of monitoring or tolerate an elaborate system of electrodes that impedes normal activity. Towards this end, we designed and implemented a simple, reliable system architecture based on a wearable ECG sensing system using a single lead of ECG. We describe the wearable prototype system that we built in Section 6.2.

6.1 Data Collection

Subjects were asked to exercise on the treadmill for 12–15 minutes (training dataset DT) or 5–7 minutes (test dataset DX). We collected test and training data on different days. The subjects were told to pace themselves and slowly work up to a jog; after at least

2 minutes of brisk jogging they were asked to slow down gradually to a halt. The data is manually labeled with annotations about the subjects pace and duration of exercise. We collected sitting (DS) and recovery (DR) data immediately before and after the training work-out.

To construct the training dataset (DT, DS, DR) we selected approximately 10000 samples from each of the following activity annotations – sit, walk, run, endure run and recover. These are grouped into either three activity level annotations: sit+recover (labeled: still), walk (labeled: low intensity), run+endure run (labeled: high intensity) or two activity levels annotations: sit+recover (labeled: still) and walk+run+endure run (labeled: high+low intensity) for the supervised models. Some subjects had fewer than 10,000 samples per annotation due to noise. In aggregate the training dataset size for each subject ranged between 40,000-50,000 samples. We tested our classifiers using samples from DX (except Table 6.1).

6.2 Prototype Application

Figure 6.1: Prototype Architecture. The SHIMMER sensor board collects ECG and accelerometer data, then sends data to Nokia N95 through Bluetooth. The mobile phone forwards the data to the authentication server through Wi-Fi. MATLAB authentication engine identifies or verifies the patient's identity using machine learning algorithms.

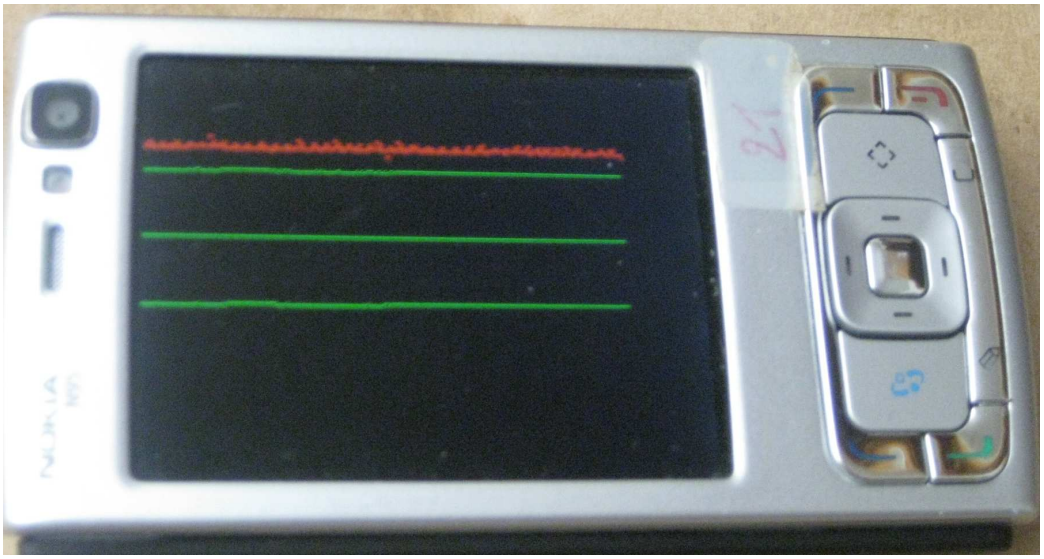

Figure 6.2: Prototype mobile application showing three channels of the triaxial accelerometer (green) and one channel of the ECG data (red). Data is scaled down to very low resolution before display. The mobile application forwards the sensor data to the authentication server for remote authentication.

To test the feasibility of our biometric verification approach, we implemented a prototype application as shown in Figure 6.1. Our primary design goal for the prototype was to set up a simple and reliable architecture to relay data from the sensor to an authentication server that runs the pattern recognition algorithms. We implemented a NesC application running on the SHIMMER to send ASCII packets of data, at the sampling rate, from the onboard accelerometer and the add-on ECG sensor board over Bluetooth [7]. A thin-client application running on a mobile phone (Nokia N95) wirelessly receives sensor data over Bluetooth and forwards it to the remote authentication server over an IEEE802.11g (Wi-Fi) link (see Figure 6.2). Our protocol forwards chunks of 4000 samples so that data is sent to the authentication server every 40s. We implemented the analysis algorithms in MATLAB. The authentication server periodically analyzed the sensor data and logged the results. It is also possible to move the trained models and subsequent computation on the phone. The current approach, however, scales better if more subjects are added. Although

this approach works, significant development and evaluation still needs to be done to make this application practical and usable.

6.3 Results and Discussion

To compare with related approaches, we first evaluate the performance of the classifiers on data taken from subjects at rest (DS). The results are presented in Table 6.1 and are comparable to other existing approaches.

	KNN	xKNN	BN
Precision	0.96	0.97	0.97
Recall	0.95	0.97	0.97

Table 6.1: Identification performance for the sitting session (DS). We randomly select 20 windows as the test dataset and the remaining data as the training dataset.

Next we tested the performances of the different activity-aware and activity-unaware classifiers on the test dataset DX. Generally, the activity-aware classifiers outperformed the activity-unaware classifiers (as shown in Table 6.2) by being able to explain the intra-subject variability seen in the ECG signal. Among the activity-aware classifiers, the KNN classifiers do not explicitly model the effects of different activity levels. Nonetheless, the simple inclusion of the additional accelerometer modality is clearly useful, as seen by the improvement in performance. We use k=1 (one neighbour) based on our results from cross-validation. The BN classifier makes better use of the accelerometer data by explicitly modeling the activities, which leads to slightly better performance numbers even with the manual activity annotations.

Manual annotations are inconvenient, unreliable, subjective and unsuitable for fine-grained activity clustering (beyond a small number of levels). We used activity labels

	Activity-Aware				Activity-Unaware		
	KNN	xKNN	BN		KNN	xKNN	BN
			$\|H\| = 2$	$\|H\| = 3$			
Precision	0.8243	0.8278	0.8488	0.8252	0.7855	0.7677	0.8139
Recall	0.8039	0.7925	0.8326	0.8174	0.8035	0.7987	0.8140

Table 6.2: Identification performance of the activity-aware classifiers against the activity-unaware classifiers. The activity-aware KNN classifiers use a concatenated feature vector of activity and ECG features. The activity-aware BN is provided supervised activity labels derived from manual annotations. An improvement is apparent even with just two activity levels.

derived from unsupervised activity clustering using Gaussian mixture models. Table 6.3 shows the performance of the Bayesian classifier based on unsupervised activity clustering. The case where $|H|$=1 corresponds to the activity-unaware classifier.

	Window Identification		Person Identification
No. of Activity Levels	True Positive Rate	False Positive Rate	Accuracy
1	81.39	5.65	14/17
2	77.59	5.63	15/17
3	78.67	5.65	15/17
4	79.34	5.57	15/17
5	78.03	5.52	15/17

Table 6.3: Identification performance for the Bayesian network classifier using unsupervised activity clustering for varying number of activity clusters. A test session consists of a sequence of ECG feature windows extracted from dataset DT. The window identification treats each feature vector as a separate test data point. The person identification decision combines results from all the windows and selects the person predicted by majority of the windows.

Table 6.4 shows the performance of verification with varying number of imposters. Verification decisions are made according to Equation(5.9). We can view the false positive

rate (FPR) as an indicator of the security of the system. As would be expected, FPR is reduced as more imposters were added to the pool. It should be noted that we evaluate the entire test dataset from all subjects against every combination of claimant and imposter to obtain the results shown in Table 6.4. When the number of imposters is large, the random sampling did not include sufficient samples from each activity and imposter combination. This resulted in an increase in false acceptances possibly due to an ill-constructed pooled dataset. With too few imposters the pooled dataset does not have enough information to begin with.

	Window Verification		Person Verification
No. of Imposters	True Positive Rate	False Positive Rate	Accuracy
3	81.68	12.72	16/17
7	81.14	11.72	16/17
8	79.31	11.13	16/17
11	81.7	12.19	17/17
15	79.85	12.06	16/17

Table 6.4: Verification performance for different sizes of imposter pools. The test dataset consists of all windows from all persons tested for every possible claimant. A person is considered correctly verified if a majority of his samples are verified as legitimate, i.e.,TPR>0.5.

Figure 6.3 shows the ROC curve for the verification model. Depending on the nature of application, we can choose to optimize for fewer false positives or more true positives by selecting different operating points on the curve .

To help reduce the number of overall false rejection, we aggregate the window verification decision. As described in Section 5.3.2, we combine 10 window predictions in an ongoing manner in our experiments. We use predictions from the 8 person imposter model. The results in Table 6.5 show, for each person, how often his identity claims are correctly accepted (legitimate claimant) and how often the claims made by the most confused im-

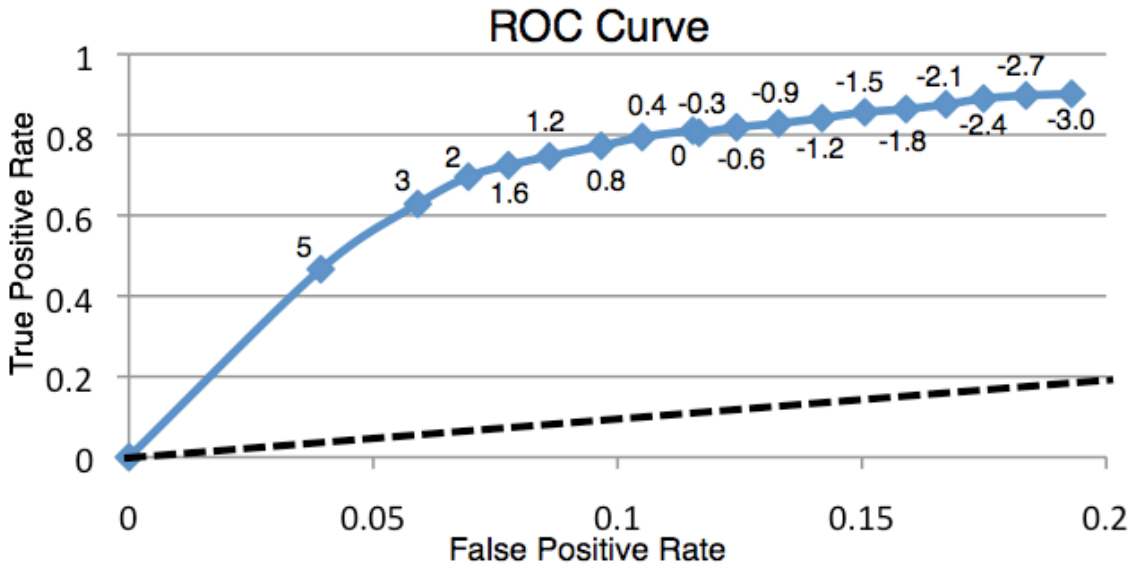

Figure 6.3: ROC curve for the verification model (8 imposters). The thresholds used are shown in the graph. We can see that with higher thresholds the system rejects too many legitimate users and with lower thresholds too many imposters are accepted. The dotted line shows y=x.

poster are accepted. The most confused imposter test provides the worst case verification numbers. Fewer imposter claims are incorrectly accepted for the other imposters in the dataset.

	Legitimate Claimant	Imposter
p1	100.00	0.00
p2	88.24	75.00
p3	90.91	0.00
p4	100.00	0.00
p5	100.00	0.00
p6	100.00	27.27
p7	81.82	0.00
p8	100.00	70.00
p9	85.71	12.50
p10	80.00	0.00
p11	81.82	0.13
p12	93.75	83.3
p13	91.67	0.00
p14	100.00	0.00
p15	77.78	0.00
p16	100.00	0.00
p17	60.00	0.00

Table 6.5: Acceptance rates for person verification (8 imposters) by aggregating window verification decisions. A person verification decision is made based on the most number of verified samples within a chunk. The test dataset consists of data from the legitimate claimant and imposter (most confused).

Chapter 7

Summary

In this thesis we introduce a biometric based on a novel combination of human electrocardiogram (ECG) and accelerometer data, and investigated its performance on 17 healthy subjects. We described algorithms for data processing, classification and clustering schemes and developed a prototype architecture to demonstrate the feasibility of our scheme. We implemented activity-aware Nearest-Neighbor and Bayesian network classifiers and compared their performances to similar classifiers which used no activity information. The findings from this work demonstrate that the human ECG coupled with activity information, is indeed a viable biometric, even in the face of activity-induced variability. In general, Bayesian networks offer an efficient and elegant way of encoding observed dependencies. Hence our proposed approach could pave the way for an ongoing mobile authentication scheme that does not require frequent and active participation from the user. Future work include a broader range of recognized activities, better approaches for combining or reasoning about classifier predictions, and addition of other sensors (for e.g., a galvanic skin response (GSR) sensor can be used to classify emotional states of the subject). Results from 17 subjects indicate that the proposed approach shows potential for biometric recognition,

however, more subjects must be added to understand the performance for a larger subject pool. Other factors such as increased physical fitness, cardiological treatments etc., could also affect the accuracy for an existing subject pool. Due to the long-term variability in the human ECG, the system may also need to be re-trained after a certain period of time. Thus, further investigation is required to understand the generality of the proposed approach.

Appendix A

Plots

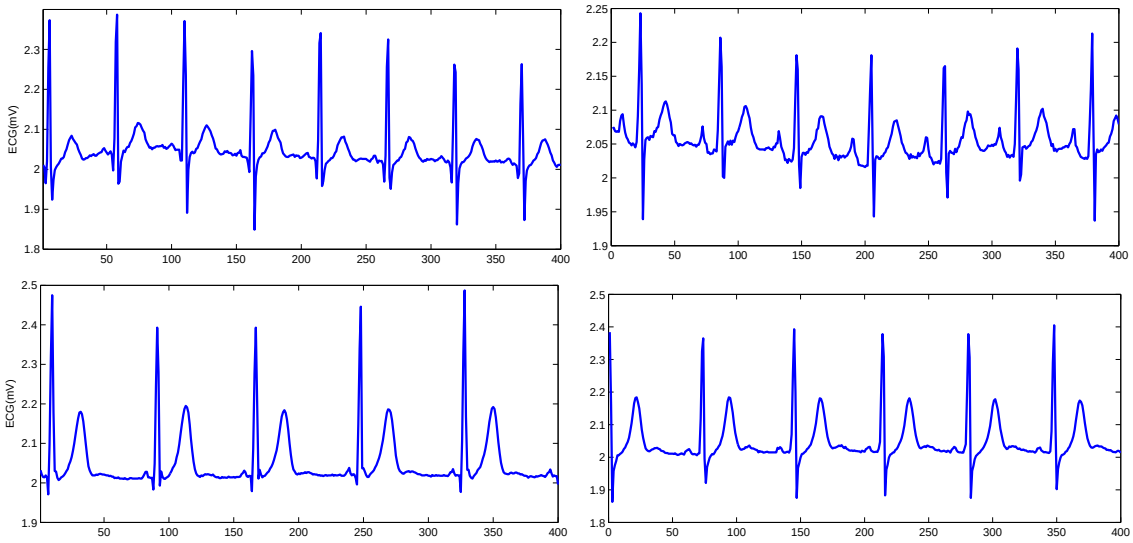

Figure A.1: Windows of ECG from four different persons. We see that the ECG windows from the different persons, while conforming to the fundamental morphology also exhibits some unique patterns.

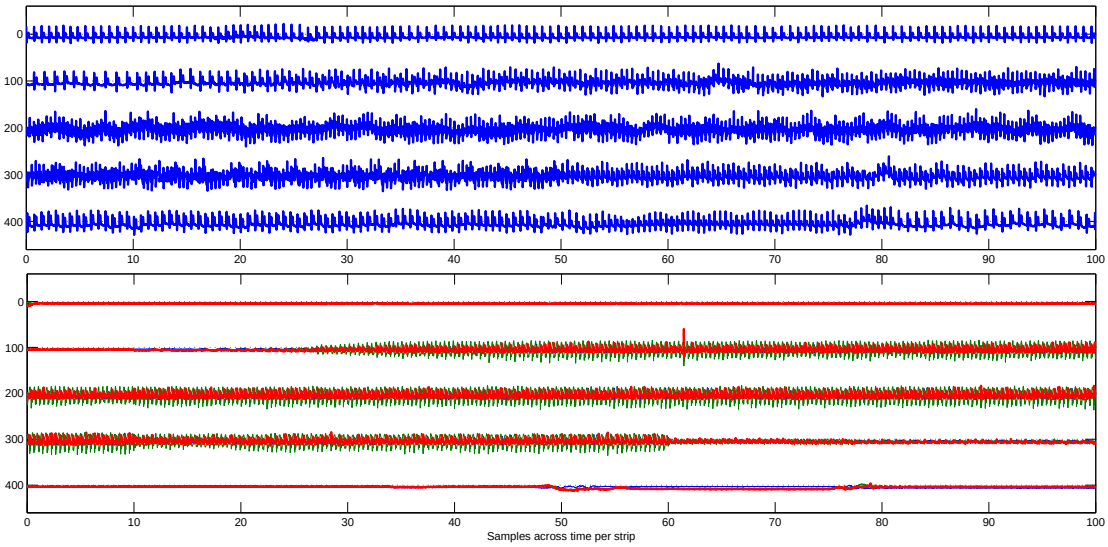

Figure A.2: Example of a training dataset from a single subject across different activities. Strips of ECG data are shown above and the corresponding strips of triaxial accelerometer data are shown below. We can observe activity induced variability in the second, third and fourth strips of 10000 samples each.

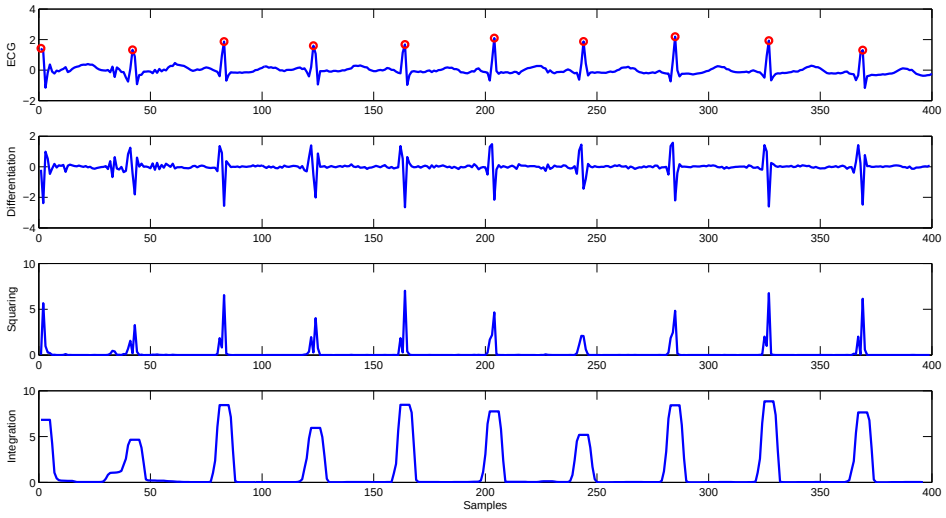

Figure A.3: QRS detection algorithm processing steps for a single ECG window (a) zero-meaned ECG signal. (detected R-peaks marked) (b) Output of differentiator. (c) Output of squaring process. (d) Results of moving-window integration.

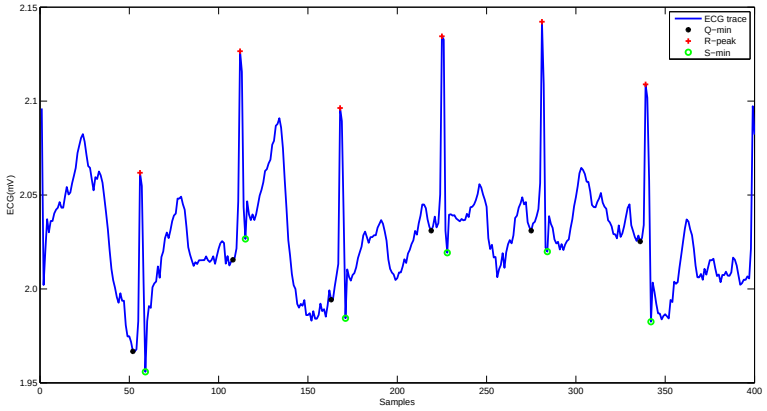

(a) Noisy Beat A

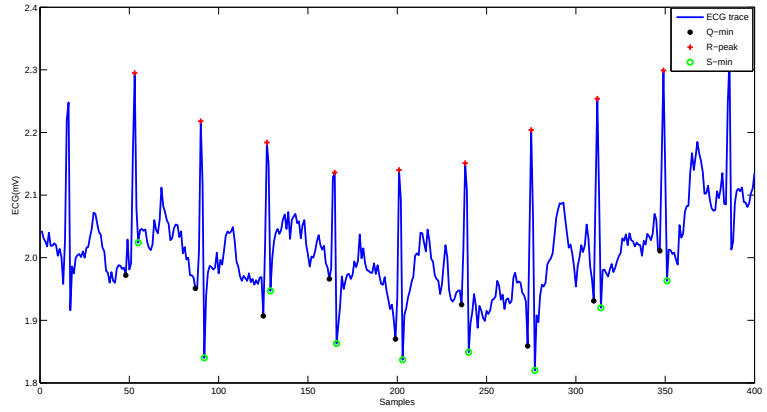

(b) Noisy Beat B

Figure A.4: The output of the QRS detector for two examples of noisy beats from different persons. We observe that the R-peaks can be located even in the presence of noise.

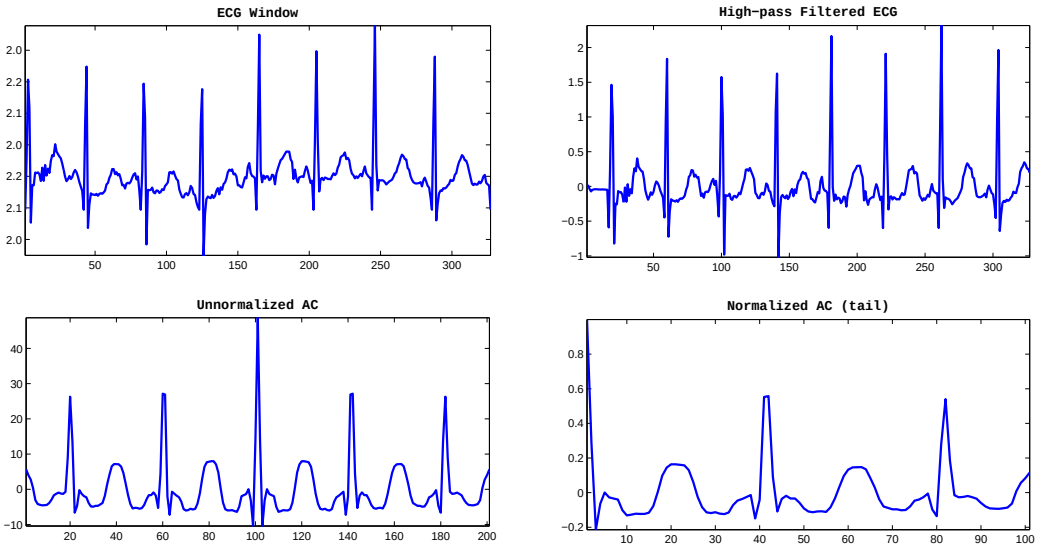

Figure A.5: Steps involved in Autocorrelation feature extraction for a single window of ECG data. The window is first baseline corrected, then high pass filtered. The resulting Autocorrelation function (only tail portion) is then normalized by the zero-lag coefficient.

Appendix B

Detailed Classification Performance

	Predictions																	
Actual	p1	p2	p3	p4	p5	p6	p7	p8	p9	p10	p11	p12	p13	p14	p15	p16	p17	Total Samples
p1	98	0	0	0	0	0	0	0	0	0	0	0	0	1	0	0	0	99
p2	0	51	3	0	0	0	0	0	0	0	0	71	2	0	12	32	5	176
p3	0	1	92	0	0	0	0	0	0	0	0	16	0	0	0	0	1	110
p4	0	0	0	50	0	0	0	0	0	0	0	0	0	0	0	0	0	50
p5	0	0	0	0	112	0	1	0	0	0	0	0	0	0	0	0	1	114
p6	0	0	6	0	0	43	0	0	0	0	0	0	0	0	0	0	0	49
p7	0	0	0	0	14	0	36	0	0	0	0	0	4	0	0	1	57	112
p8	6	0	0	0	0	0	0	25	1	0	0	0	0	5	0	0	0	37
p9	15	0	0	0	0	0	0	30	20	0	0	0	0	0	0	0	0	65
p10	0	0	0	0	0	0	0	1	3	31	0	0	0	4	0	0	6	45
p11	0	6	0	0	0	0	0	0	0	0	84	1	2	0	0	10	2	105
p12	0	2	0	0	0	0	0	0	0	0	0	160	0	0	0	1	0	163
p13	0	0	0	0	0	0	9	0	0	0	1	1	88	0	0	0	17	116
p14	0	0	0	0	0	0	0	0	0	0	0	0	0	77	0	0	1	78
p15	0	0	0	0	0	0	0	0	0	0	0	0	2	0	77	3	3	85
p16	2	0	0	0	0	0	0	0	0	0	0	0	0	0	0	77	1	80
p17	1	0	0	0	0	0	0	0	0	0	0	0	2	6	0	1	37	47

Table B.1: Confusion Matrix - Activity-Unaware ($|H| = 1$).

	Predictions																	
Actual	p1	p2	p3	p4	p5	p6	p7	p8	p9	p10	p11	p12	p13	p14	p15	p16	p17	Total Samples
p1	97	0	0	0	0	0	0	0	0	0	0	0	0	2	0	0	0	99
p2	0	81	1	0	0	2	0	0	0	0	0	49	3	0	16	16	8	176
p3	0	12	87	0	0	3	0	0	0	0	0	5	1	0	2	0	0	110
p4	0	0	0	50	0	0	0	0	0	0	0	0	0	0	0	0	0	50
p5	0	0	0	0	113	0	1	0	0	0	0	0	0	0	0	0	0	114
p6	0	0	0	0	0	49	0	0	0	0	0	0	0	0	0	0	0	49
p7	0	0	0	0	3	0	32	0	0	0	0	0	7	0	0	0	70	112
p8	7	0	0	0	0	0	0	24	0	0	0	0	0	6	0	0	0	37
p9	26	0	0	0	0	0	0	25	14	0	0	0	0	0	0	0	0	65
p10	0	0	0	0	0	0	0	2	0	34	0	0	0	5	0	0	4	45
p11	0	4	0	0	0	0	0	0	0	0	87	0	2	0	0	9	3	105
p12	0	10	0	0	0	0	0	0	0	0	0	153	0	0	0	0	0	163
p13	0	0	0	0	0	0	10	0	0	0	1	1	88	0	0	1	15	116
p14	0	0	0	0	0	0	0	0	0	0	0	0	0	77	0	0	1	78
p15	0	0	0	0	0	0	0	0	0	0	0	0	1	0	78	4	2	85
p16	1	0	0	0	0	0	0	0	0	0	0	0	0	1	0	77	1	80
p17	1	0	0	0	0	0	0	0	0	0	0	0	2	6	0	0	38	47

Table B.2: Confusion Matrix - GMM based activity clustering, 2 activity levels.

	Predictions																	
Actual	p1	p2	p3	p4	p5	p6	p7	p8	p9	p10	p11	p12	p13	p14	p15	p16	p17	Total Samples
p1	98	0	0	0	0	0	0	0	0	0	0	0	0	1	0	0	0	99
p2	0	88	3	0	0	1	0	0	0	0	1	62	0	0	6	8	7	176
p3	0	16	85	0	0	3	0	0	0	0	0	6	0	0	0	0	0	110
p4	0	0	0	50	0	0	0	0	0	0	0	0	0	0	0	0	0	50
p5	0	0	0	0	112	0	1	0	0	0	0	0	0	0	0	0	1	114
p6	0	0	0	0	0	49	0	0	0	0	0	0	0	0	0	0	0	49
p7	0	0	0	0	3	0	43	0	0	0	0	0	4	0	0	0	62	112
p8	5	0	0	0	0	0	0	26	0	0	0	0	0	6	0	0	0	37
p9	12	0	0	0	0	0	0	32	21	0	0	0	0	0	0	0	0	65
p10	0	0	0	0	0	0	0	0	1	40	0	0	0	2	0	0	2	45
p11	0	1	0	0	0	0	0	0	0	0	91	4	1	0	0	5	3	105
p12	0	17	0	0	0	0	0	0	0	0	0	146	0	0	0	0	0	163
p13	0	1	0	0	2	0	32	0	0	0	4	1	66	0	0	0	10	116
p16	0	0	0	0	0	0	0	1	0	0	0	0	0	76	0	0	1	78
p17	0	2	0	0	0	0	0	0	0	0	0	4	0	0	71	2	6	85
p18	1	0	0	0	0	0	0	0	0	0	0	0	0	1	0	76	2	80
p19	0	0	0	0	0	0	0	0	0	0	0	0	2	7	0	1	37	47

Table B.3: Confusion Matrix - GMM based activity clustering, 5 activity levels.

	$h = 1$		$h = 2$		$h = 3$		$h = 4$		$h = 5$	
	Precision	Recall	Precision	Recall	Precision	Recall	Precision	Recall	Precision	Recall
p1	0.803	0.990	0.735	0.980	0.836	0.980	0.845	0.990	0.845	0.990
p2	0.850	0.290	0.757	0.460	0.716	0.443	0.639	0.483	0.704	0.500
p3	0.911	0.836	0.989	0.791	0.989	0.818	0.940	0.718	0.966	0.773
p4	1.000	1.000	1.000	1.000	1.000	1.000	1.000	1.000	1.000	1.000
p5	0.889	0.982	0.974	0.991	0.902	0.974	0.974	0.991	0.957	0.982
p6	1.000	0.878	0.907	1.000	0.925	1.000	0.942	1.000	1.000	1.000
p7	0.783	0.321	0.744	0.286	0.569	0.259	0.544	0.330	0.566	0.384
p8	0.446	0.676	0.471	0.649	0.407	0.649	0.394	0.703	0.441	0.703
p9	0.833	0.308	1.000	0.215	0.955	0.323	0.947	0.277	0.955	0.323
p10	1.000	0.689	1.000	0.756	1.000	0.778	1.000	0.844	1.000	0.889
p11	0.988	0.800	0.989	0.829	0.968	0.876	0.969	0.886	0.948	0.867
p12	0.643	0.982	0.736	0.939	0.699	0.926	0.675	0.853	0.655	0.896
p13	0.880	0.759	0.846	0.759	0.866	0.612	0.857	0.569	0.904	0.569
p14	0.828	0.987	0.794	0.987	0.792	0.974	0.826	0.974	0.817	0.974
p15	0.865	0.906	0.812	0.918	0.906	0.906	0.846	0.906	0.922	0.835
p16	0.616	0.963	0.720	0.963	0.733	0.963	0.776	0.950	0.826	0.950
p17	0.282	0.787	0.268	0.809	0.266	0.809	0.279	0.766	0.282	0.787
Mean	0.80105	0.77369	0.80828	0.78407	0.79575	0.78172	0.7914	0.77884	0.80659	0.78952

Table B.4: Identification performance using the Bayesian network for 1 to 5 activity levels, GMM-based activity clustering. The shaded boxes represent the activity level at which maximum precision and recall occur. We try to highlight the same activity level for both maximum values.

	Claim																	
Actual	p1	p2	p3	p4	p5	p6	p7	p8	p9	p10	p11	p12	p13	p14	p15	p16	p17	Total Samples
p1	99	0	0	28	0	0	0	61	7	0	0	0	0	4	0	0	0	99
p2	0	113	1	0	0	1	0	0	0	0	1	126	0	0	62	37	2	176
p3	0	46	78	0	0	7	0	0	0	0	0	8	0	0	2	0	0	110
p4	7	0	0	50	0	0	0	50	0	1	0	0	0	0	0	0	0	50
p5	0	0	1	0	109	41	21	0	0	0	1	0	2	0	0	0	86	114
p6	0	0	30	0	1	49	0	0	0	0	0	19	0	0	0	1	1	49
p7	0	17	1	0	10	13	58	0	0	0	0	17	43	0	0	15	35	112
p8	25	0	0	25	0	0	0	32	14	0	0	0	0	32	0	0	0	37
p9	65	0	0	11	0	0	0	63	50	0	0	0	0	0	0	0	0	65
p10	0	0	0	0	0	0	0	4	2	27	0	0	0	0	0	0	0	45
p11	0	3	0	0	0	0	0	0	0	0	83	21	15	0	8	21	1	105
p12	0	113	0	0	0	0	0	0	0	0	15	156	0	0	85	44	0	163
p13	0	8	2	0	1	0	54	0	0	0	3	2	100	0	3	33	70	116
p14	2	0	0	0	0	0	0	4	1	0	0	0	0	75	0	0	0	78
p15	0	20	0	0	0	0	0	0	0	0	0	21	0	0	52	7	1	85
p16	3	16	0	0	0	0	0	0	0	0	6	23	0	2	0	76	3	80
p17	1	0	0	0	0	0	0	0	0	0	0	0	0	2	1	1	20	47

Table B.5: Confusion Matrix - Verification using 8 imposters and maximum likelihood estimation. Values show the number of samples verified for a particular actual person/claimed person combination.

Bibliography

[1] F. Agrafioti and D. Hatzinakos. Fusion of ECG sources for human identification. In *Proceedings of the 3rd International Symposium on Communications, Control and Signal Processing, ISCCSP 2008*, pages 1542–1547, March 2008.

[2] J. Ashbourn. *Biometrics: advanced identity verification*. Springer-Verlag London, 2000.

[3] Abhilasha Bhargav-Spantzel, Anna Squicciarini, and Elisa Bertino. Privacy preserving multi-factor authentication with biometrics. In *DIM '06: Proceedings of the second ACM workshop on Digital identity management*, pages 63–72, 2006.

[4] L. Biel, O. Pettersson, L. Philipson, and P. Wide. ECG analysis: a new approach in human identification. In *Proceedings of the 16th IEEE Instrumentation and Measurement Technology Conference*, volume 1, pages 557–561, 1999.

[5] Frédéric Bimbot, Jean-François Bonastre, Corinne Fredouille, Guillaume Gravier, Ivan Magrin-Chagnolleau, Sylvain Meignier, Teva Merlin, Javier Ortega-García, Dijana Petrovska-Delacrétaz, and Douglas A. Reynolds. A tutorial on text-independent speaker verification. *EURASIP J. Appl. Signal Process.*, 2004:430–451, 2004.

[6] BioMOBIUS. As viewed Jul 2009. `http://www.biomobius.org/`.

[7] Bluetooth Special Interest Group. Specification of the Bluetooth System: Core V2.1 + EDR, July 2007.

[8] BNT. As viewed Jul 2009. `http://www.cs.ubc.ca/~murphyk/Software/BNT/bnt.html`.

[9] A. D. C. Chan, M. M. Hamdy, A. Badre, and V. Badee. Wavelet distance measure for person identification using electrocardiograms. *IEEE Transactions on Instrumentation and Measurement*, 57(2):248–253, February 2008.

[10] C. V. Chan and D. R. Kaufman. Mobile phones as mediators of health behavior change in cardiovascular disease in developing countries. *Studies in Health Technology and Informatics*, 143:453–458, 2009.

[11] C. Chiu, C. Chuang, and C. Hsu. A novel personal identity verification approach using a discrete wavelet transform of the ECG signal. In *Proceedings of the International Conference on Multimedia and Ubiquitous Engineering, MUE 2008*, pages 201–206, April 2008.

[12] G. D. Clifford, F. Azuaje, and P. McSharry. *Advanced methods and tools for ECG data analysis*. Artech House, Inc., 2006.

[13] G.D. Clifford and L. Tarassenko. Quantifying errors in spectral estimates of hrv due to beat replacement and resampling. *Biomedical Engineering, IEEE Transactions on*, 52(4):630–638, April 2005.

[14] Douglas A. Coast, Richard M. Stern, Gerald G. Cano, and Stanley A. Briller. An approach to cardiac arrhythmia analysis using hidden markov models. *IEEE Transactions on Biomedical Engineering*, 37(9):826–836, Sep 1990.

[15] I. G. Damousis, D. Tzovaras, and E. Bekiaris. Unobtrusive multimodal biometric authentication: The HUMABIO project concept. *EURASIP Journal on Advances in Signal Processing*, 2008:1–11, 2008.

[16] I. Daskalov and I. Christov. Improvement of resolution in measurement of electrocardiogram rr intervals by interpolation. *Medical Engineering & Physics*, 19(4):375 – 379, 1997.

[17] Alexander P. Derchak and Lance Myers. SYSTEM AND METHOD FOR IDENTITY CONFIRMATION USING PHYSIOLOGIC BIOMETRICS TO DETERMINE A PHYSIOLOGIC FINGERPRINT, August 2007.

[18] D di Bernardo, P Langley, and A Murray. Effect of changes in heart rate and in action potential duration on the electrocardiogram t wave shape. *Physiological Measurement*, 23(2):355–364, 2002.

[19] N. J. Fortuin and J. L. Weiss. Exercise stress testing. *Journal of the American Heart Association*, 56(5):699–712, 1977.

[20] Ernest Frank. An accurate, clinically practical system for spatial vectorcardiography. *Circulation*, 13(5):737–749, 1956.

[21] FTC. Federal trade commission survey on identity theft. Web site, as viewed Jun 2009, 2003.

[22] LS Green, RL Lux, CW Haws, RR Williams, SC Hunt, and MJ Burgess. Effects of age, sex, and body habitus on qrs and st-t potential maps of 1100 normal subjects. *Circulation*, 71(2):244–253, 1985.

[23] Y. Y. Gu, Y. Zhang, and Y. T. Zhang. A novel biometric approach in human verification by photoplethysmographic signals. In *Proceedings of the 4th Annual IEEE Conference on Information Technology Applications in Biomedicine, UK*, pages 13–14, April 2003.

[24] Y. Y. Gu, Y. Zhang, and Y. T. Zhang. Biometric statistical study of one-lead ecg features and body mass index (bmi). In *Proceedings of the 2005 IEEE Engineering in Medicine and Biology 27th Annual Conference*, pages 1162–1165, 2005.

[25] R. Hoekema, G. J. H. Uijen, and A. van Oosterom. Geometrical aspects of the interindividual variability of multilead ECG recordings. *IEEE Transactions on Biomedical Engineering*, 48(5):551–559, May 2001.

[26] S. A. Israel, J. M. Irvine, A. Cheng, M. D. Wiederhold, and B. K. Wiederhold. ECG to identify individuals. *Pattern Recognition*, 38(1):133–142, January 2005.

[27] S. A. Israel, W. T. Scruggs, W. J. Worek, and J. M. Irvine. Fusing face and ECG for personal identification. In *Proceedings of the 32nd Applied Imagery Pattern Recognition Workshop*, pages 226–231, October 2003.

[28] Franc Jager, Roger G. Mark, George B. Moody, and Saga Divjak. Analysis of transient st segment changes during ambulatory monitoring using the karhunen-loeave transform. pages 691–694, Oct 1992.

[29] H.A. Kestler, A. Muller, V. Hombach, J. Wohrle, O. Grebe, G. Palm, M. Moher, and F. Schwenker. Decision fusion of micro-variability and signal averaged ecg parameters from the qrs complex with rbf networks. pages 297–300, Sep 2002.

[30] H. S. Kim and H. S. Jeong. A nurse short message service by cellular phone in type-2 diabetic patients for six months. *Journal of Clinical Nursing*, 16(6):1082–1087, June 2007.

[31] Andrew J. Klosterman and Gregory R. Ganger. Secure continuous biometric-enhanced authentication. Technical report, CMU, May 2000.

[32] Sandeep Kumar, Terence Sim, Rajkumar Janakiraman, and Sheng Zhang. Using continuous biometric verification to protect interactive login sessions. In *ACSAC '05: Proceedings of the 21st Annual Computer Security Applications Conference*, pages 441–450, 2005.

[33] A. G. Logan, W. J. McIsaac, A. Tisler, M. J. Irvine, A. Saunders, A. Dunai, C. A. Rizo, D. S. Feig, M. Hamill, M. Trudel, and J. A. Cafazzo. Mobile phone-based remote patient monitoring system for management of hypertension in diabetic patients. *American Journal of Hypertension*, 20(9):942–948, September 2007.

[34] A. Lymberis. Smart wearables for remote health monitoring, from prevention to rehabilitation: current R&D, future challenges. In *Proceedings of the 4th International IEEE EMBS Special Topic Conference on the Information Technology Applications in Biomedicine*, pages 272–275, April 2003.

[35] C. Maier, H. Dickhaus, M. Bauch, and T. Penzel. Comparison of heart rhythm and morphological ecg features in recognition of sleep apnea from the ecg. pages 311–314, Sep 2003.

[36] M Malik, P Farbom, V Batchvarov, K Hnatkova, and A J Camm. Relation between qt and rr intervals is highly individual among healthy subjects: implications for heart rate correction of the qt interval. *Heart*, 87(3):220–228, 2002.

[37] Tsutomu Matsumoto, Hiroyuki Matsumoto, Koji Yamada, and Satoshi Hoshino. Impact of artificial "gummy" fingers on fingerprint systems. In *Society of Photo-Optical Instrumentation Engineers (SPIE) Conference Series*, volume 4677 of *Presented at the Society of Photo-Optical Instrumentation Engineers (SPIE) Conference*, pages 275–289, April 2002.

[38] M. Milanesi1, N. Martini, N. Vanello, V. Positano, M. F. Santarelli, and L. Landini. Independent component analysis applied to the removal of motion artifacts from electrocardiographic signals. *Medical and Biological Engineering and Computing*, 46:251–261, 2008.

[39] MIT. MIT-BIH database of MIT. Project web site, as viewed March 2009.

[40] University of Washington. Assisted Cognition project at UW. Project web site, as viewed March 2008.

[41] NSTC Subcommittee on Biometrics. Privacy & biometrics building a conceptual foundation, September 2006.

[42] Jiapu Pan and Willis J. Tompkins. A real-time QRS detection algorithm. *Biomedical Engineering, IEEE Transactions on*, 32(3):230–236, March 1985.

[43] Costas Papaloukas, Dimitrios I. Fotiadis, Aristidis Likas, and Lampros K. Michalis. An ischemia detection method based on artificial neural networks. *Artificial intelligence in medicine*, 24(2):167–178, Feb 2002.

[44] K. N. Plataniotis, D. Hatzinakos, and J. K. M. Lee. ECG biometric recognition without fiducial detection. *Biometrics Symposium: Special Session on Research at the Biometric Consortium Conference*, 19:1–6, August 2006.

[45] Salil Prabhakar, Sharath Pankanti, and Anil K. Jain. Biometric recognition: Security and privacy concerns. *IEEE Security and Privacy*, 1(2):33–42, 2003.

[46] Shankara Reddy Qiuzhen Xue. Algorithms for computerized qt analysis. *Journal of electrocardiology*, 30:181–186, Jan 1998.

[47] M. A. D. Raya and L. G. Sison. Adaptive noise cancelling of motion artifact in stress ECG signals using accelerometer. In *Proceedings of the Second Joint EMBS/BMES Conference*, volume 2, pages 1756–1757, 2002.

[48] Intel Research. Digital Home project at Intel. Project web site, as viewed March 2008.

[49] Brian A. Barsky Richard H. Bartels, John C. Beatty. *An introduction to splines for use in computer graphics and geometric modeling*. Morgan Kaufmann, 3 edition, 1995.

[50] A. E. Rosenberg and S. Parthasarathy. Speaker background models for connected digit password speaker verification. In *ICASSP '96: Proceedings of the Acoustics, Speech, and Signal Processing, 1996. on Conference Proceedings., 1996 IEEE International Conference*, pages 81–84, 1996.

[51] Hussein I. Shahein and Hazem M. Abbas. Ecg data compression via cubic-splines and scan-along polygonal approximation. *Signal Process.*, 35(3):269–283, 1994.

[52] T. W. Shen, W. J. Tompkins, and Y. H. Hu. One-lead ECG for identity verification. *Proceedings of the 24th Annual Conference Engineering in Medicine and Biology and the Annual Fall Meeting of the Biomedical Engineering Society, EMBS/BMES Conference*, 1:62–63, 2002.

[53] W. Shen. *Biometric identity verification based on electrocardiogram (ECG)*. PhD thesis, University of Wisconsin, Madison, 2005.

[54] T. Sim, Sheng Zhang, R. Janakiraman, and S. Kumar. Continuous verification using multimodal biometrics. *IEEE Transactions on Pattern Analysis and Machine Intelligence*, 29(4):687–700, April 2007.

[55] M. L. Simoons and P. G. Hugenholtz. Gradual changes of ECG waveform during and after exercise in normal subjects. *Journal of the American Heart Association*, 52:570–577, 1975.

[56] D. A. Tong, K. A. Bartels, and K. S. Honeyager. Adaptive reduction of motion artifact in the electrocardiogram. In *Proceedings of the Second Joint EMBS/BMES Conference*, volume 2, pages 1403–1404, 2002.

[57] Y. Wang, F. Agrafioti, D. Hatzinakos, and K. N. Plataniotis. Analysis of human electrocardiogram for biometric recognition. *EURASIP Journal on Advances in Signal Processing*, 2008(1):1–6, 2008.

[58] Annika Welinder, Leif Sornmo, Dirk Q. Feild, Charles L. Feldman, Jonas Pettersson, Galen S. Wagner, and Olle Pahlm. Comparison of signal quality between easi and mason-likar 12-lead electrocardiograms during physical activity. *American Journal of Critical Care*, 13(3):228–234, 2004.

[59] Mark D. Wiederhold, Steven A. Israel, Rodney P. Meyer, and John M. Irvine. Identification by analysis of physiometric variation, January 2006.

[60] G. Wuebbeler, R. Bousseljot, D. Kreiseler, M. Stavridis, and C. Elster. Human verification by heart beat signals, working group 8.42, physikalisch-technische bundesanstalt(PTB), berlin, germany, 2004.